UNIVERSITATEA BABEŞ-BOLYAI
BABEŞ-BOLYAI TUDOMÁNYEGYETEM
BABEŞ-BOLYAI UNIVERSITÄT
BABEŞ-BOLYAI UNIVERSITY
TRADITIO ET EXCELLENTIA

FACULTATEA DE FIZICĂ
Str. Mihail Kogălniceanu nr.1
Cluj-Napoca, RO-400084
Tel: +4(0)264-405300 | FAX: +4(0)264-591906
secretariat.phys@ubbcluj.ro
www.phys.ubbcluj.ro

PhD. Thesis

- summary -

STUDY OF MATERIALS PROPRIETIES USED AS SUPPORT FOR LOCAL DOSE CONTROL IN EXTERNAL BEAM RADIOTHERAPY

Andreea – Cosmina CIOBANU

Scientific coordinator

Prof.dr. Zoltán BÁLINT

Cluj-Napoca

2025

ABSTRACT

This thesis proposes the manufacturing of 3D-printed boluses to address air gaps in radiotherapy, which can lead to overdose of skin tissues or underdosing of tumours. By using 3D-printing technology, the thesis aims to create a model of bolus that fit the patient anatomy, reducing air gaps and improving the delivered dose. This not only solves air gaps but also improves the overall quality of treatment, optimizing tumour management and reducing side effects to healthy tissues.

The research focuses on the choice of suitable materials and their performance in dosimetric assessments, with the aim of developing a consistent technique for testing bolus materials that may be included in clinical practice. The thesis aims to contribute to the development of tailored radiation approaches that increase patient safety and treatment efficacy by addressing air gaps and exploring creative ideas.

However, the study notes some limitations, such as the need for specific knowledge in planning and designing boluses, printing process time, supply chain problems, and a small spectrum of appropriate materials for radiation. Addressing these limitations is important for the full recognition of the advantages of 3D-printed bolus solutions in clinical settings.

1. CHAPTER 1 – RADIOTHERAPY INSIGHTS

Boluses are mandatory in particular cases of cancer treated using high-energy radiotherapy for efficient dose distribution. However, traditional boluses can introduce air gaps, affecting treatment outcomes. Researchers are exploring the use of custom boluses and the impact of different materials on dose distribution using electron beam radiotherapy. 3D-printing, a technique that creates physical models with specific shapes from digital information, offers advantages such as less waste, low cost, and individualized design. The use of 3D-printed boluses in radiotherapy has seen a significant increase in research interest over the past 15 years, with published articles on 3D printing, bolus, and radiotherapy increasing from 10 in 2001 to 204 in 2024. This trend highlights the potential of 3D printing to improve radiotherapy treatments' precision and effectiveness.

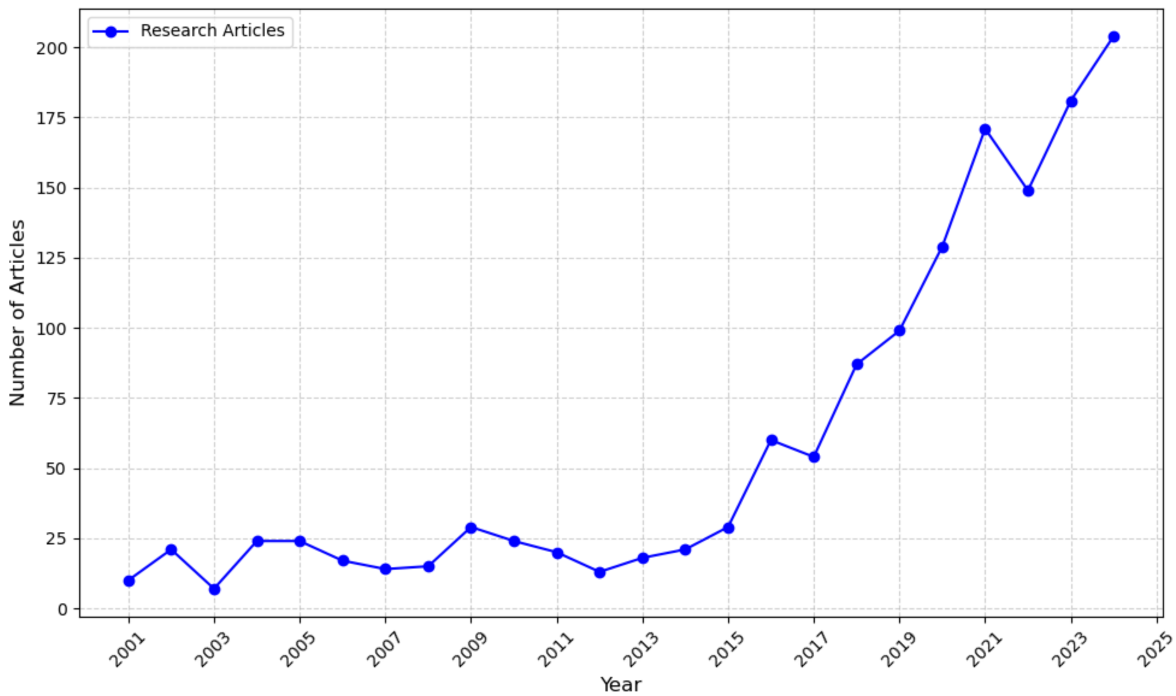

Figure 1.1 – Number of Research Articles Published in the Last 15 Years (Science Direct Database)

Bolus materials are essential in radiotherapy for various cancer treatments, including post-mastectomy chest wall irradiation, skin involvement, and high risk of recurrence in superficial tissues. International clinical guidelines suggest the use of bolus for increasing surface dose coverage in chest wall irradiation and skin cancers. 3D-printed boluses have shown promise in delivering an adequate therapeutic dose to superficial tissues, improving skin contact with patients and simplifying treatment planning. Patient-specific 3D-printed boluses have shown improved skin contact with patients, making them an alternative to commercial options. Mesh boluses have minimal effect on depth-dose profiles but increase surface dose, simplifying treatment planning. Wang et al.'s (2021) research emphasizes the importance of selecting appropriate bolus materials based on the specific treatment case to safeguard deep tissues during electron beam radiotherapy. However, there are still issues to overcome, such as precise bolus fit and air gap avoidance. Advancements in 3D-printing technology, materials, and integration into workflow could counterbalance these limits and make 3D-printed boluses possible in radiation therapy.

1.1.Profile depth dose (PDD) for tumors

The Medical Linear Accelerator (LINAC) is a radiation treatment option for cancer or tumours, aiming to deliver the highest dose possible while preserving healthy cells close to the tumour. The dose distribution must be precise to achieve the therapeutic goal. The percentage depth dose (PDD) and dose profile are two variables to be checked before using LINAC. PDD indicates the amount of the highest dose deposited compared to the total dose, and is affected by factors like source to surface distance, field size, beam energy, and depth of interest. For cases like skin cancer or superficial tumours, the highest dose should be found under the skin.

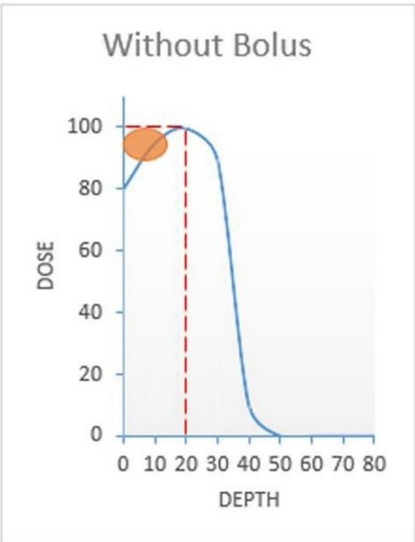

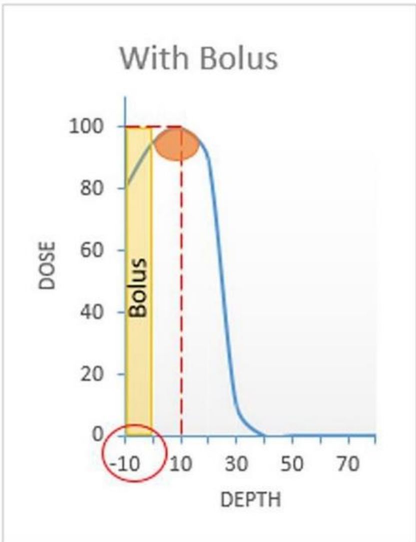

Figure 1.2 – Bolus impact on build-up area of profile depth doses

The orange area represents tumours where optimal build-up dose is for treatment. Photon beam incidence modifies dose distribution, requiring corrections to isodose charts. Attenuation of photons near patient contours may cause unintended changes to isodose curves at depth.

1.2.Dose compensators in radiotherapy

Airgaps in radiotherapy can lead to underdosing of a target area, especially in superficial tumors. These gaps allow radiation beams to pass through without depositing energy in the tumor, causing inadequate tumor control and increased recurrence risk. Correct placement of bolus and avoiding airgaps is demanded for optimal treatment outcomes. Compensators are high-attenuation materials used in radiation therapy to adjust the intensity of radiation beams. They are custom-fabricated for each patient and beam configuration and do not increase skin dose. Wedges are high-attenuation materials used to alter the distribution of isodose lines, typically placed on the treatment head of a linear accelerator. Modern linear accelerators use dynamic wedges, which reduce the dose like a physical wedge. Boluses are used when the patient's contour is irregular, making a wedge insufficient. Compensators are made from materials that can effectively attenuate radiation beams while maintaining structural integrity and biocompatibility. Common materials include tissue-equivalent materials, metals, and polymers. Tissue-equivalent materials are preferred due to their close resemblance to human tissue, while metals like lead and tungsten are effective but can be dangerous. The choice of compensator materials must balance performance, safety, and cost-effectiveness to improve outcomes.

1.3.The 3D-Printing alternative and biocompatibility

3D-printing technology has revolutionized radiation therapy by enabling the making of patient-specific bolus materials. It also aids in the development of patient-specific immobilization devices, ensuring reproducibility and stability during treatment. Research on biocompatibility of 3D-printed materials like Polylactic Acid (PLA), Thermoplastic Polyurethane (TPU), and resin has shown their suitability for radiation therapy applications. PLA is suitable for 3D-printing radiation therapy phantoms and is an equivalent substitute for soft human tissue in MV photon radiation dosimetry and therapy. TPU, with its good tear and abrasion resistance, is used in 3D-printing for patient-specific immobilization devices. PLA and TPU offer the potential to optimize rigidity and flexibility, depending on clinical requirements. Additionally, resin materials provide high resolution and smooth surface finishes for precise models. Biocompatibility and material suitability for radiation therapy are being researched using 3D-printed materials, however, considering the different properties of materials should not be avoided. This might be quantified by several factors such as the structural properties of the materials, changes in their chemical structure under radiation, or the use of additives during filament production line processes that have an impact on the biocompatibility.

2. CHAPTER 2 - 3D CONCEPT VALIDATION

This chapter examines six materials for 3D-printed boluses in radiation therapy, aiming to identify the most effective solution for clinical applications. Commercial boluses have limitations, such as not adhering to unique anatomical differences between patients. 3D-printing technology can create boluses that fit specific anatomical features, ensuring they have physical properties similar to human tissue and can impact radiation without affecting dose distribution. Challenges include finding an appropriate area for bolus placement in the LINAC treatment field and designing a bolus holder to securely hold samples under radiation exposure.

Validation methods

The decision on filament type used was based on biocompatibility first, which ensures that the used materials will not have adverse effects on human tissue while in contact. Moreover, the chosen filaments must have a density that corresponds to human skin, as the appropriate dose distribution and radiation absorption depends on this. Literature showed up many suitable materials for evaluation: ABS (Acrylonitrile Butadiene Styrene), ASA (Acrylonitrile Styrene Acrylate), Premium PLA (PLA-P), Polycarbonate, Standard PLA (PLA-S), and PET-G (Polyethylene Terephthalate Glycol-Modified). These materials allow us to evaluate their properties and performance to identify the best suitable filament for 3D-printed boluses in radiation applications.

Table 2.1 - Density and dimension values for commercial bolus and 3D-Printing filaments

	Material	Density (g/cm^3)	Dimension (cm)
1.	Commercial Bolus	1.02	30 x 30 x 0.5
2.	PLA-Standard	1.24	21.5 x 21.5 x 0.5
3.	PLA-Premium	1.17	21.5 x 21.5 x 0.5
4.	ABS	1.04	21.5 x 21.5 x 0.5
5.	Polycarbonate	1.19	21.5 x 21.5 x 0.5
6.	ASA	1.07	21.5 x 21.5 x 0.5
7.	PET-G	1.27	21.5 x 21.5 x 0.5

Commercial bolus sheets are 30 cm x 30 cm, but we set a 20 cm x 20 cm field at the accelerator to measure profile depth doses. Bolus samples were printed at 21.5 cm x 21.5 cm and 0.5 cm thickness, comparing 3D-printed bolus performance to commercial criteria.

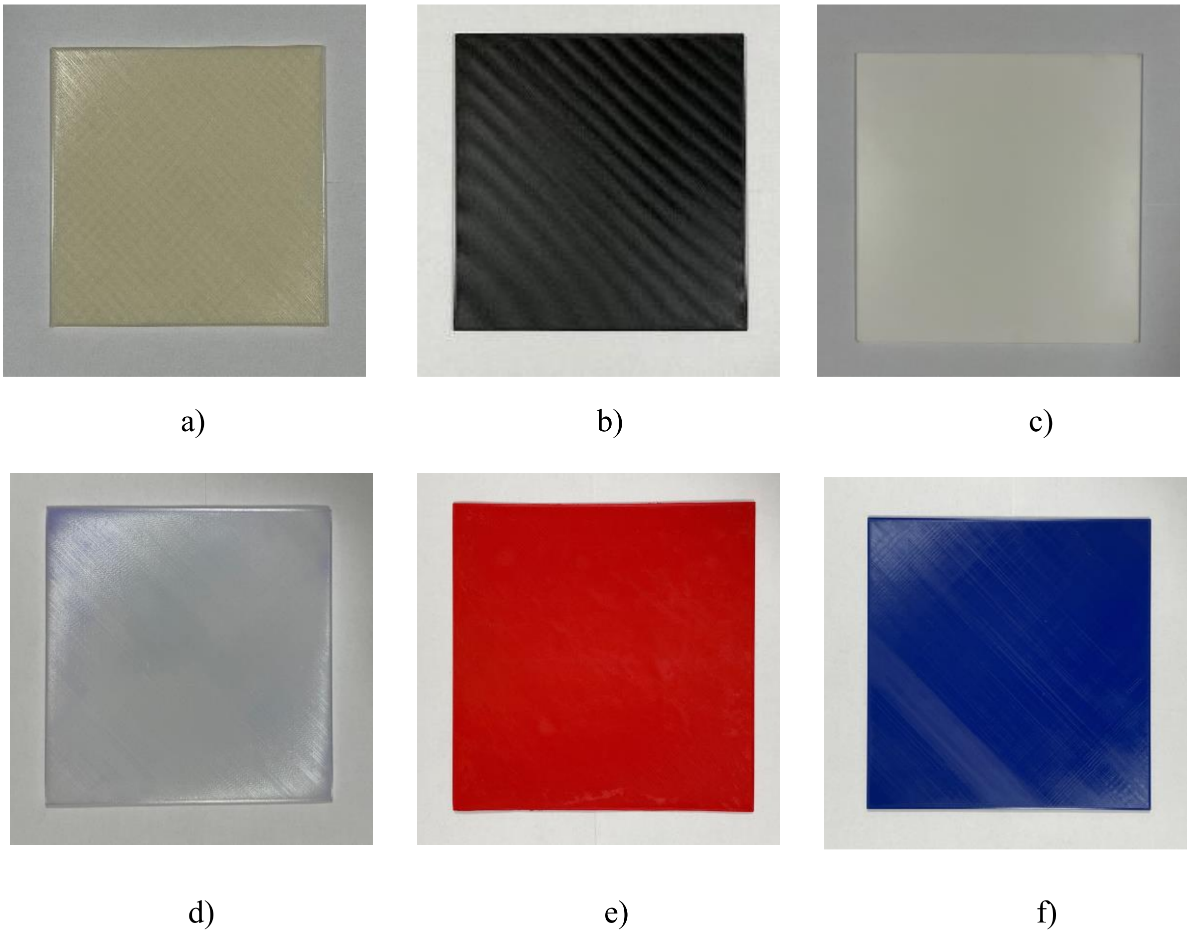

Figure 2.1 – Printed bolus plates samples as following: a) Premium PLA; b) Standard PLA; c) ABS; d) Polycarbonate; d) ASA; e) PET-G

The study utilized Autodesk Inventor Professional 2021 (Autodesk, San Rafael, California); for prototyping and Ultimate Cura 4.5 (Ultimaker, Zaltbommel, Netherlands) for printing and parameterizing. Two printers, Flashforge Guider II (Zhejiang Flashbourne 3D technology Co. LTD) and Creality CR-10S PRO V2 (Shenzhen Creality 3D Technology Co. LTD), were used for testing materials, with the latter being a more advanced option. Both tools were used for professional-grade 3D-CAD design.

2.1.Hounsfield Units (HU) test

Hounsfield Units (HU) are vital for material density and composition comparisons. However, standard deviations can be high due to factors like beam hardening artifacts, heterogeneity of scanned material, and differences in acquisition parameters, reconstruction algorithms, and scanner calibration. Noise and artifacts in CT images also contribute to fluctuation. The size and shape of the ROIs also affect the standard deviation.

The study focused on choosing six filaments based on their density, similar to human tissue, and comparing their radiation attenuation values with commercially used boluses. CT scans were used to validate the materials, and the results showed that ABS, ASA, PLA-P, Polycarbonate, PLA-S, and PET-G filaments had higher HU values than commercial boluses. This data was used to validate the materials' fit for clinical use.

2.2. Profile depth doses test

The study used a Varian True Beam linear accelerator, water tank phantom, electrometer, and ionization chamber to produce clinical results, ensure radiation exposure, and examine bolus sample influence, comparing 3D-printed samples with commercial scans. Accurate data on percentage depth dose distributions is crucial for determining patient dose from medical exposure. The study examined the correlation between building material density and PDDs, observing expansion of air gaps and displacement of buildup area. PDD is determined by depth, field size, and SD.

Table 2.2 - Ds variation depending on field width

Material	$D_{s\ (5\times5)}$ (%)				$D_{s\ (10\times10)}$ (%)			
Airgap (cm)	0	0.5	1	1.5	0	0.5	1	1.5
Commercial Bolus	95.59	94.18	89.55	88.02	96.32	94.76	91.66	90.49
ABS	89.12	88.98	88.88	86.47	91.54	90.8	90.35	90.24
ASA	86.51	86.06	85.25	83.90	89.07	88.78	88.64	87.83
Premium PLA	90.98	90.75	90.57	90.14	92.75	92.78	92.77	92.49
Polycarbonate	88.55	87.87	86.09	85.49	90.41	89.75	89.68	89.7
Standard PLA	89.15	88.80	88.35	88.32	92.36	91.89	91.76	91.11
PET-G	88.78	88.73	88.62	87.63	92.29	92.18	92.07	91.68
	$D_{s\ (15\times15)}$ (%)				$D_{s\ (20\times20)}$ (%)			
Airgap (cm)	0	0.5	1	1.5	0	0.5	1	1.5
Commercial Bolus	97.26	95.43	92.65	91.75	97.94	96.21	93.53	92.70
ABS	92.99	92.80	92.57	92.23	93.99	93.62	92.95	92.54
ASA	90.36	90.12	89.66	89.60	91.92	91.83	91.70	91.23
Premium PLA	94.15	94.10	93.88	93.81	95.45	95.28	95.97	95.75
Polycarbonate	92.31	92.18	91.85	91.62	94.06	92.86	92.83	92.71
Standard PLA	93.48	92.92	92.56	92.39	93.92	93.82	93.70	93.68

PET-G	93.92	93.43	93.23	92.84	95.10	95.03	94.36	94.28

2.3.Absolute dose measurements

The test aimed to compare the surface dose buildup power of 3D filament materials using solid water slabs. New equipment and re-scanning of bolus samples were used to validate data. Three dose measurements were recorded for each material, using a solid water slab and commercial bolus as reference. This extra validation process ensured the materials met clinical application criteria. The experimental setup used a beam geometry with a source-to-surface distance of 100 cm and various field widths for irradiation raging from 6x6 to 14x14 cm. 100MU was irradiated at a constant dose rate, maintaining ideal conditions of 22.9°C temperature and 101.77 kPa pressure. Measurements were taken using the Farmer FC23-C ionization chamber and the DOSE2 electrometer (IBA Dosimetry, Schwarzenbruck, Germany), with the chambers used for PDD observations not requiring charge recombination adjustment.

Table 2.3 - Mean dose values in nC in build-up region for commercial bolus, solid water slab and 3D filaments

	6 x 6 (cm)	8 x 8 (cm)	10 x 10 (cm)	14 x 14 (cm)
Solid Water	9.172	9.392	9.555	9.792
Standard-PLA	9.181	9.397	9.564	9.791
Premium-PLA	9.174	9.398	9.566	9.798
ABS	9.201	9.416	9.581	9.825
Polycarbonate	9.156	9.376	9.543	9.776
ASA	9.217	9.432	9.593	9.829
PET-G	9.192	9.407	9.573	9.805

The graph shows that the ASA and PC materials show a high sensitivity to irradiation, compromising the expected results in terms of build-up region. As a result, two materials can be excluded from the six examined, allowing for further testing for the remaining four materials.

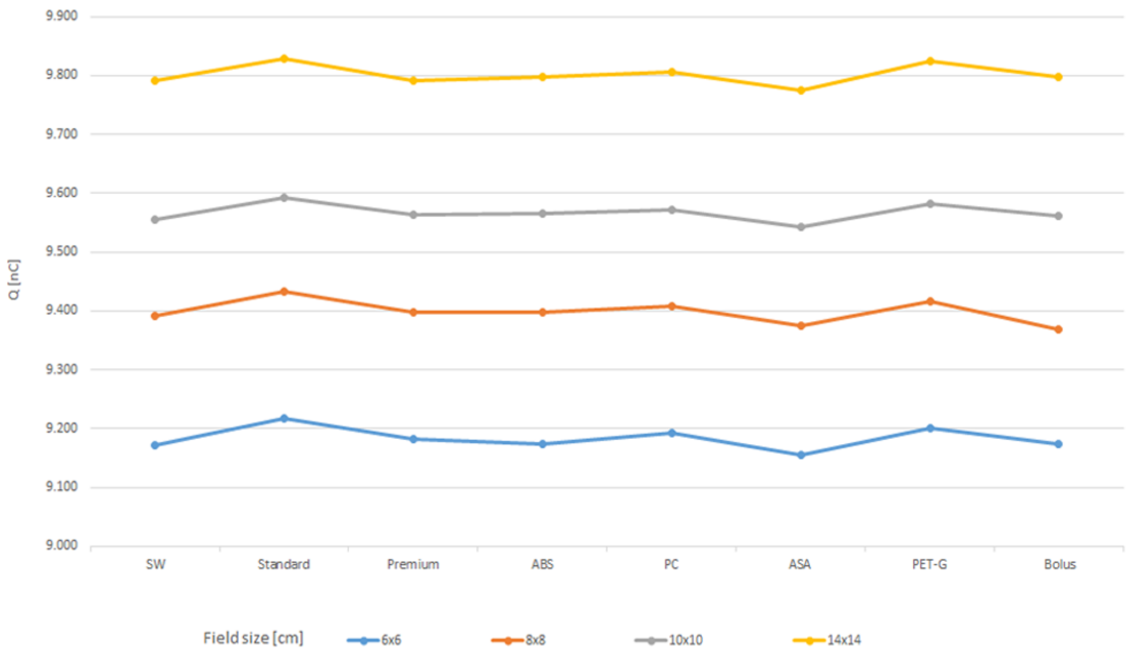

Figure 2.2 - Dose variation dependency for different irradiation field sizes and materials

2.4.Measured dose vs calculated dose

The validation method confirms materials in a treatment planning system using solid water slabs and CT images, determining dose profiles and percentage depth dose.

The processed data included statistical analysis to evaluate the concordance between measured and calculated doses from a dosimetric perspective. Figure 2.3 shows exported values to assess the significance of the area beneath the dose curve for the build-up region of each 3D bolus.

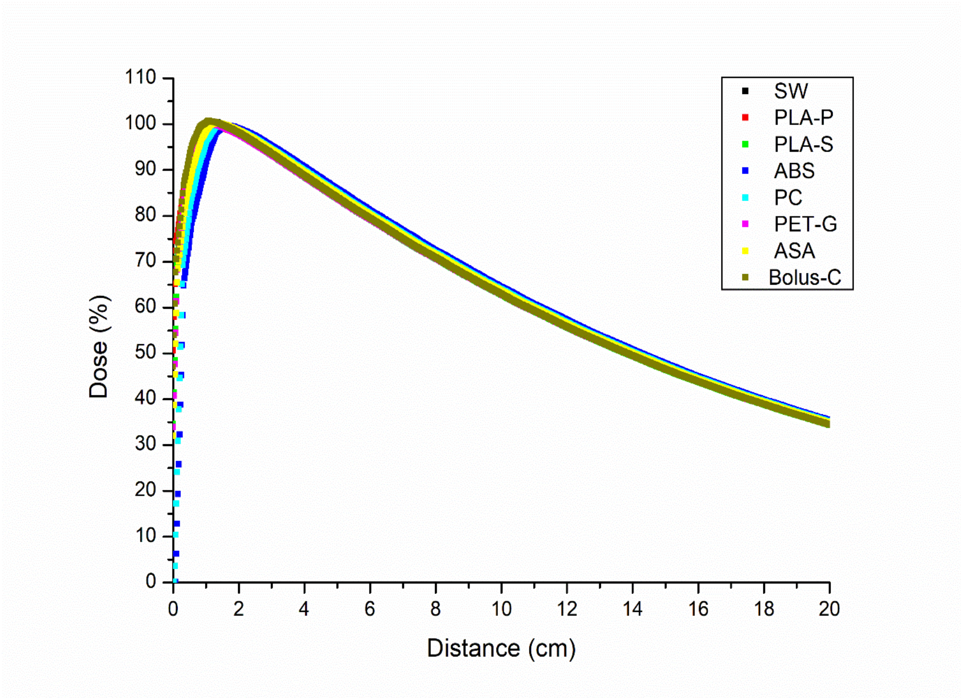

Figure 2.3 - Exported TPS PDDs values for each material

For each profile, peak, height and area values are presented and analysed in Table 2.4, as follows:

Table 2.4 - values for area, peak and height

	Area	Peak	Height	Area diff.	Peak diff.	Height diff.
Bolus-C	1300.00	1.08	100.65			
SW	1301.98	1.10	100.57	1.97	0.02	0.08
PLA-S	1294.09	1.13	100.16	5.91	0.05	0.49
PET-G	1294.40	1.13	99.96	5.60	0.05	0.69
PLA-P	1299.12	1.33	99.65	0.88	0.25	1.00
ASA	1304.53	1.38	100.25	4.52	0.30	0.41
PC	1295.67	1.53	99.75	4.33	0.45	0.90
ABS	1296.95	1.58	99.71	3.05	0.50	0.94

The ABS material was deemed unsuitable for the dosimetric investigation, and it will not be included in future validation tests. The concordance correlation coefficient (ρc) was used to analyze the dataset, indicating how well observations align with the 45° line passing through the origin. The PDD curve was influenced by the bolus's proximity to the water surface, with deeper maximum doses in the build-up area. As the field size increased, the depth dose percentage decreased due to scattering factors.

Table 2.5 - Bolus plates statistical study: concordance correlation coefficient

	C. Bolus & SW	C. Bolus & PLA-S	C. Bolus & PET-G	C. Bolus & PLA-P	C. Bolus & ASA	C. Bolus & PC	C. Bolus & ABS
Concordance correlation coefficient	0.9997	0.9987	0.9984	0.9994	0.9963	0.9499	0.937
95% Confidence interval	0.9996 - 0.9997	0.9985 - 0.9989	0.9981 -0.9986	0.9993 - 0.9995	0.9957 - 0.9968	0.9431 - 0.9650	0.9280 - 0.9449
Pearson ρ (precision)	0.9997	0.9988	0.9985	0.9995	0.9964	0.9495	0.9371
Bias correction factor C_b (accuracy)	1	0.9999	0.9999	0.9999	0.9999	0.9999	0.9999

CT scans revealed that various materials, including ABS, ASA, PLA-P, Polycarbonate, PLA-S, and PET-G, have similar attenuation characteristics to commercial bolus used in clinical practice. However, ASA and PC materials were more sensitive to radiation, making them less useful for build-up regions. PLA-Premium, PLA-Standard, and PET-G were found to be the best materials for 3D printing bolus. The choice of material depends on financial implications and the simplicity of the printing procedure. PLA-Standard is the most economical choice, offering reliable performance without technical complexities. While PLA-Premium and PET-G showed good attenuation properties, their high costs may make them less suitable for clinical applications. The combined effects of performance, cost, and user-friendliness will determine the most suitable material for 3D-printed bolus applications in radiotherapy.

This part of the thesis was presented at several conferences, showcasing the research findings and contributing to the scientific dialogue in the field of radiation therapy. The oral presentation titled *"Dosimetric Impact of Bolus Airgaps for Clinical 6MV and 10MV Photon Beam"* was presented at the Innovation and Multidisciplinarity in Cancer Treatment - Congress of the Romanian Radiotherapy Society held in Sinaia from October 13-16, 2022. *"Bolus Thickness Influence in Chest Wall Radiotherapy: Comparative Study for No Bolus, 0.5 cm Bolus and 1 cm Bolus,"* was presented at the Medical and Scientific Days of the Oncological Institute Bucharest in Bucharest from May 04-07, 2023. Additionally, an oral poster presentation titled *"The Effect of Filament Density on the Build-Up Region Responsiveness of 3D Printed Boluses in High-Energy Photon Radiotherapy"* was showcased at the ASTRO Congress in San Diego, California, from October 1-4, 2023. The findings from this research were published in the International Journal of Radiation Oncology, Biology, Physics (Volume 117, Issue 2, Supplement, Page e657; DOI: 10.1016/j.ijrobp.2023.06.2089). Furthermore, a related paper titled *"Exploring the Impact of Filament Density on the Responsiveness of 3D-Printed Bolus Materials for High-Energy Photon Radiotherapy"* was published in the European Journal of Medical Physics (DOI: 10.1016/j.ejmp.2024.104849; Accepted October 22, 2024; Published online November 1, 2024; IF 3.3; AIS 0.677).

3. CHAPTER 3 - PROOF OF CONCEPT STUDY

Customized bolus on anthropomorphic phantom

This chapter discusses the development and testing of a 3D-bolus model on an anthropomorphic phantom that closely resembles human anatomy. The goal was to see if a 1:1 scale 3D-bolus could interact with radiation like commercial options. PLA-Standard was used as the main option due to its previous validation tests. Researchers developed novel solutions to address air gaps, such as a handmade bolus that conforms to patient facial contours. 3D-customized boluses have shown promise for improving fit and reducing air gaps, especially for treating head and neck cancer. The phantom was scanned and immobilized with a thermoplastic mask, comparing it to common boluses and a reference scan without a bolus. The 3D-printed bolus model was tested for dose distribution and performance, with diffraction using BeOSL detectors. The results showed good results for dose distribution, leading to better personalized radiotherapy solutions in the long run.

3.1.Setup and phantom scan

The RT Safe Prime Phantom, developed by RTsafe P.C. in Athens, Greece, mimics the anatomical structures and tissue equivalent characteristics of the human body. It serves as a solid foundation for simulating clinical scenarios and allows for validation of the proposed bolus design performance in conditions that correspond to treatment circumstances. The bolus under development is a tailored 3D-printed eye patch designed to reduce air gaps and adapt to the complex morphology of the eye area. This method evaluates the possibilities of printing boluses for irregular anatomical regions and illustrates the potential of 3D-printing techniques to meet clinical needs in challenging areas.

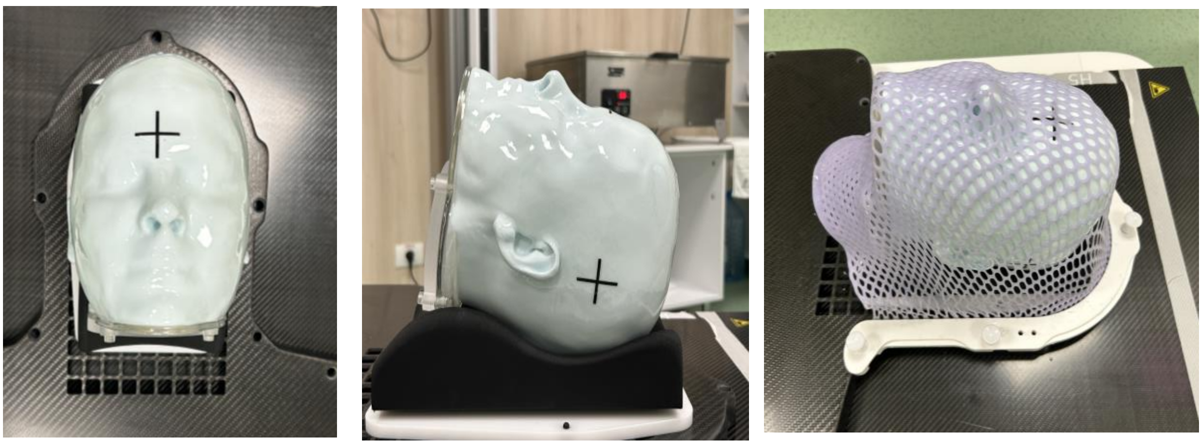

Figure 3.1 – a) top view; b) lateral view; c) phantom positioning and immobilization

A Siemens Somatom go.Top CT scan was performed on the phantom head to ensure that the scanned data is both accurate and reliable, with a scanning protocol that has a resolution of 1.25 mm.

3.2.Technical details of customized printing procedure

The phantom scan in DICOM format was converted into a 3D file using 3D Slicer software. The resulting 3D format was STL (stereolithography), with a linear tolerance of 0.125 mm. The CT scanner was designed to maintain a general tolerance of ±0.1-2 mm, depending on the nominal length and angular dimensions. To achieve accurate results, a workflow was set up to minimize major changes to the 3D model. The model was a human head with curved and non-planar surfaces made of triangles. To achieve a tighter tolerance, the STL file needed a higher resolution. The engineering standard DIN ISO 2768 provides a general tolerance of ±0.1-2 mm and angular dimensions of ±1°-0°5'.

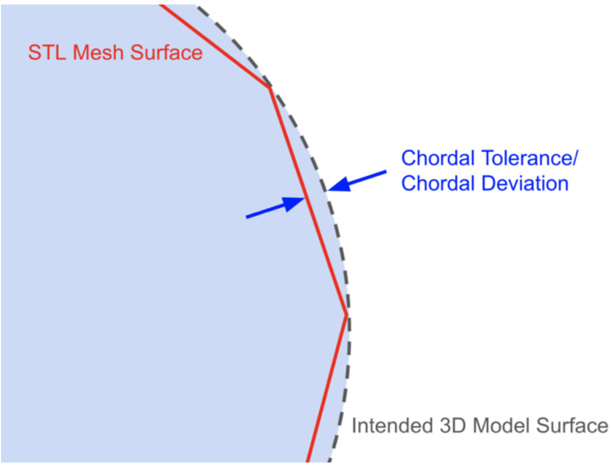

Figure 3.2 - Chordal tolerance/deviations in a circular mesh surface

Autodesk Fusion 360 was used as software for the reconstruction of the bolus surface. Although a mesh-oriented software such as Blender, Rhino, or MeshLab could have been employed for this purpose, it would not have yielded superior precision compared to a computer-aided design (CAD) modelling software. To import a mesh into Fusion 360, a plane was cut through the object to remove extra objects (Figure 3.3a). A re-mesh operation was performed based on the layer-line scan topology (Figure 3.3b), with settings like uniform type, 0.25 density, and boundary preservation. This resulted in a smoother mesh surface while maintaining the averaged mesh points. The final aspects of the object are shown in Figure 3.3c.

Table 3.1 - DICOM processing values

Name	Value
Length	153.421 mm
Width	213.82 mm
Height	210.165 mm
Facet count	549.630 (before remesh 1.253.034)
Vertex count	301.658 (before remesh 653.360)
Sheel count	16.419

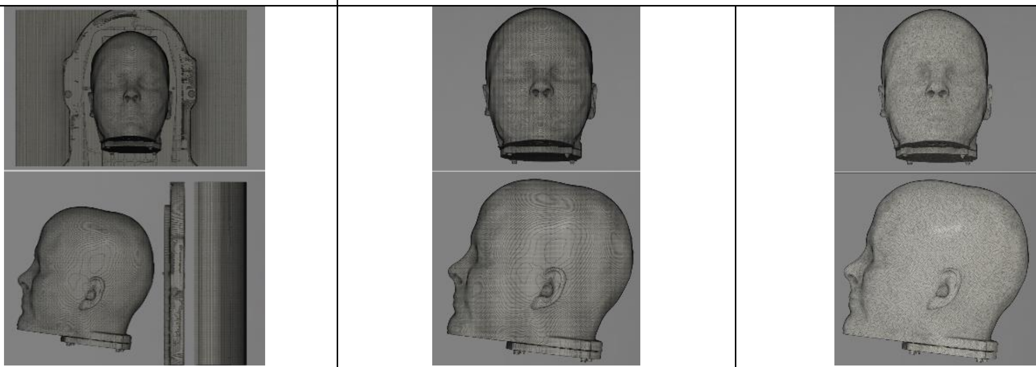

a) b) c)

Figure 3.3 - a) Original object; b) object after planar cut; c) object after smoothing

The succeeding step involves modelling the bolus within the Form environment of Fusion 360. As mentioned, conducting a direct mesh editing of the object would not yield accurate bolus dimensions. Similarly, employing an engineering CAD approach, such as sketching lines on the mesh and converting them to a 2D drawing, is insufficient due to the curved surface of the head. Forms environment can generate organic T-Splines shapes with tools that function as sculpting clay. The modelling procedure made 562 faces, all of which were quad type and were all in the right bolus area. To make sure the dimensions were as accurate as possible and to have the face width and length as uniform as possible, the vertex points were moved to line up with the mesh surface. It was conceivable to make a copy of the surfaces and move all of the spots 5.00 mm away from the original surface. The last step was to combine the surfaces created in the Forms environment to make a solid object. Figure 3.4 shows that the model is now ready to be sent to the 3D printer slicer software.

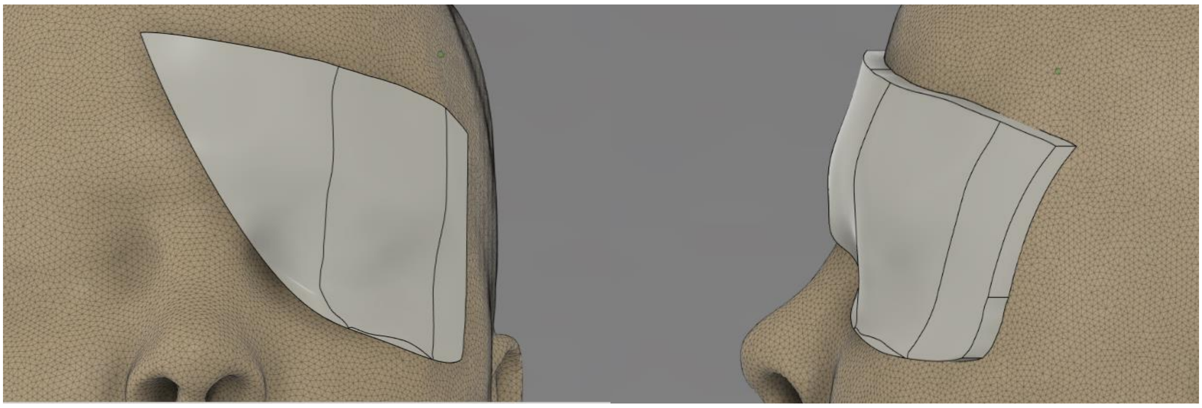

Figure 3.4 - 3D-printer slicer software bolus model export

Prior to importing the 3D STL file into the printing slicer software, an additional check was performed using 3D Slicer. This involved overlapping the bolus and phantom, as designed in Fusion 360, with both exported as a single object.

The printer utilized for the printing process was the Bambu X1 Carbon, which features a closed enclosure. The recommended slicer software for this printer, as per the manufacturer's suggestion, was Bambu Studio. To prevent any printing failures, an extra pillar was added in front of the bolus.

The final bolus patch resulted in a piece of 0.5cm thickness, like the commercially available options (Figure 3.5).

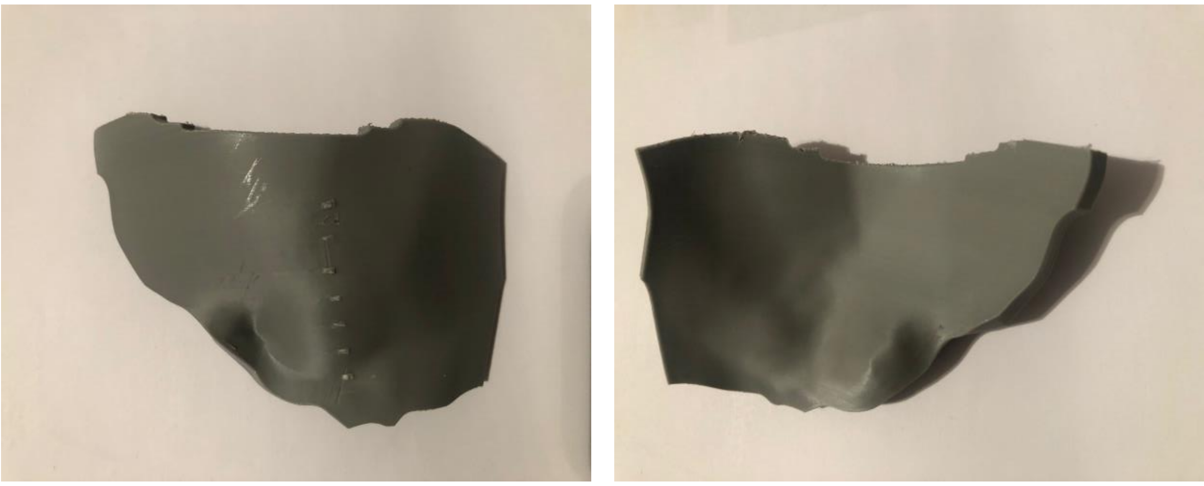

Figure 3.5 - Printed bolus (front and back view)

3.3.Positioning, scanning, and planning process

Three boluses were examined during the validation phase: a custom-built 3D-printed bolus, a commercial skin-type bolus, and a commercial thermoplastic bolus. A thermoplastic mask was used to ensure accuracy. All boluses were 0.5 cm thick and covered the left eye area of a Prime Phantom.

a) b) c)

Figure 3.6 – On phantom: a) 3D bolus; b) skin-type bolus and c) thermoplastic bolus setup

Imported scans into Eclipse Treatment Planning System was used to prepare treatment plans for each designed bolus.

3.4.Quality Assurance for bolus scans

It can be observed that the air gaps are present in all three scanned scenarios. A Hounsfield units test can be applied as a quality assurance test in order to verify the presence of air in between the bolus and phantom. It was inserted an airgap volume inside the water slabs to test the behaviour of boluses that don't fit precisely and cause air gaps in order to create a relationship between HU values and airgap distances. Water slabs setup is designed model circumstances in which there might be air gaps between the bolus and the phantom surface. Three distinct examples when the bolus does not precisely match the phantom are highlighted by the provided Hounsfield Unit (HU) differences, which show the existence of these air gaps. The configurations (Figure 3.7 A - upper row) and HU profiles (Figure 3.7 B - bottom row) for the setup with all three boluses and water slabs are presented. The profiles value in relation to our introduced airgap is shown in Figure 3.7a). Figures 3.7b), c), and d) show how airgaps behave in relation to HU units. The air volume between the bolus and the phantom has a direct impact on the values.

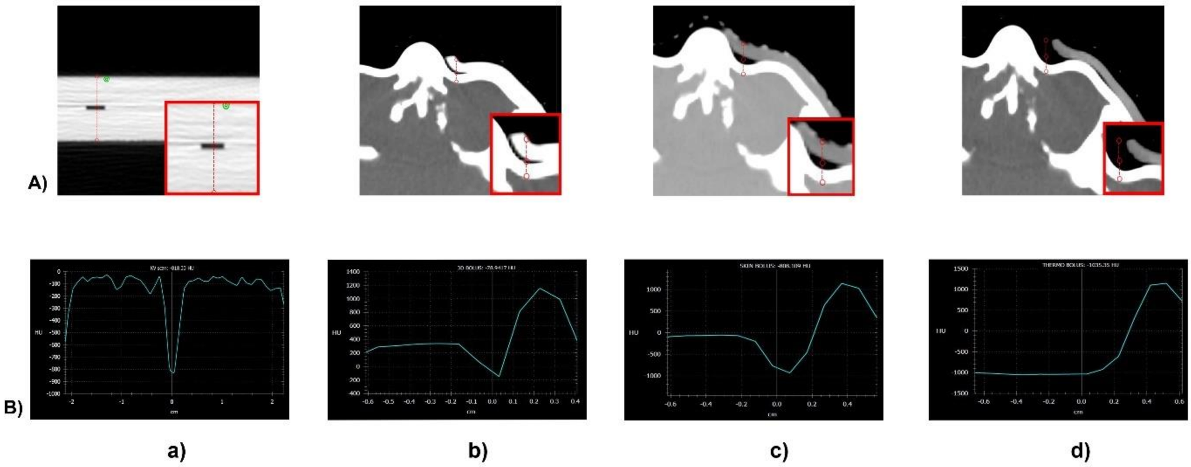

Figure 3.7 - A) Setup and positioning; B) Hounsfield Unit profiles for: a) solid water slabs; b) 3D-printed bolus; c) skin type bolus; d) thermoplastic bolus

TPS Profiles

For each set of boluses, TPS is capable of creating PDDs that will serve as a basis for our upcoming statistical analysis. Figure 3.8 displays the PDDs from the TPS for all three boluses.

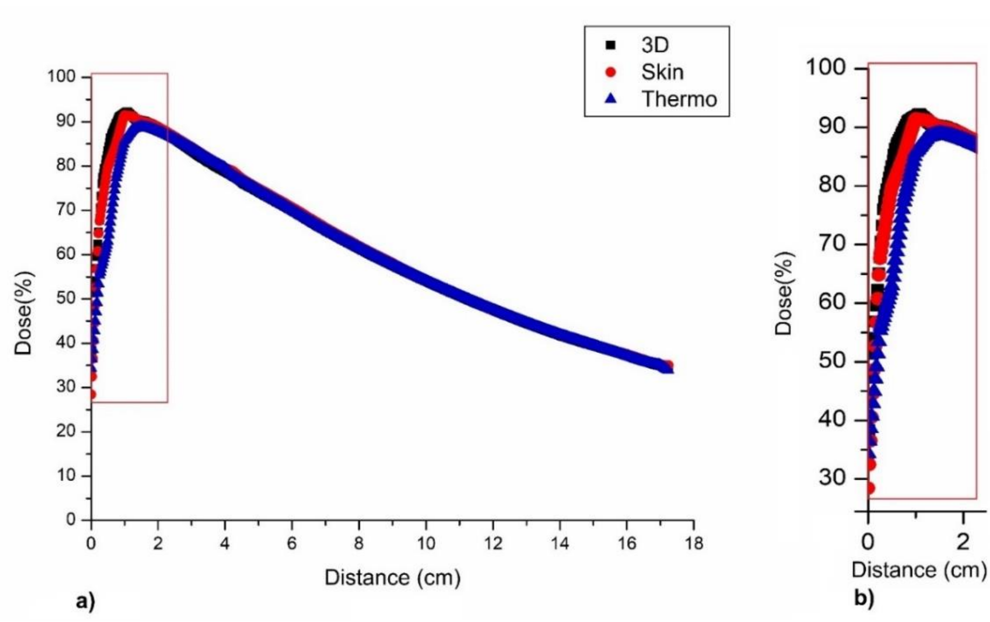

Figure 3.8 - TPS PDDs build-up area

A study comparing profile depth doses for three types of boluses to the TPS reference found that poorly fitting boluses, particularly thermoplastic boluses, failed to perform effectively. The Concordance Correlation Coefficient (ρc) increased as the air gap between the bolus surface and phantom increased, indicating a negative correlation. The 3D-printed bolus had a ρc coefficient of 0.9406, while the commercial skin bolus had a value of 0.9566. The commercial thermoplastic bolus had a value of 0.9878. The 3D-printed bolus outperformed in surface attachment and conformation to the anatomical curvature of the phantom compared to the skin type and thermoplastic boluses. Thermoplastic boluses can be difficult to reheat multiple times without losing properties, while gel boluses tend to fit better in terms of minimizing air gaps.

3.5.Dosimetric investigation with BeOSL detectors

BeOSL detectors were used for quality control and dosimetric validation, comparing irradiation and identifying inconsistencies. The study determined the actual expected dose inside the phantom head by positioning it at two distinct spots, illustrating the dose distribution.

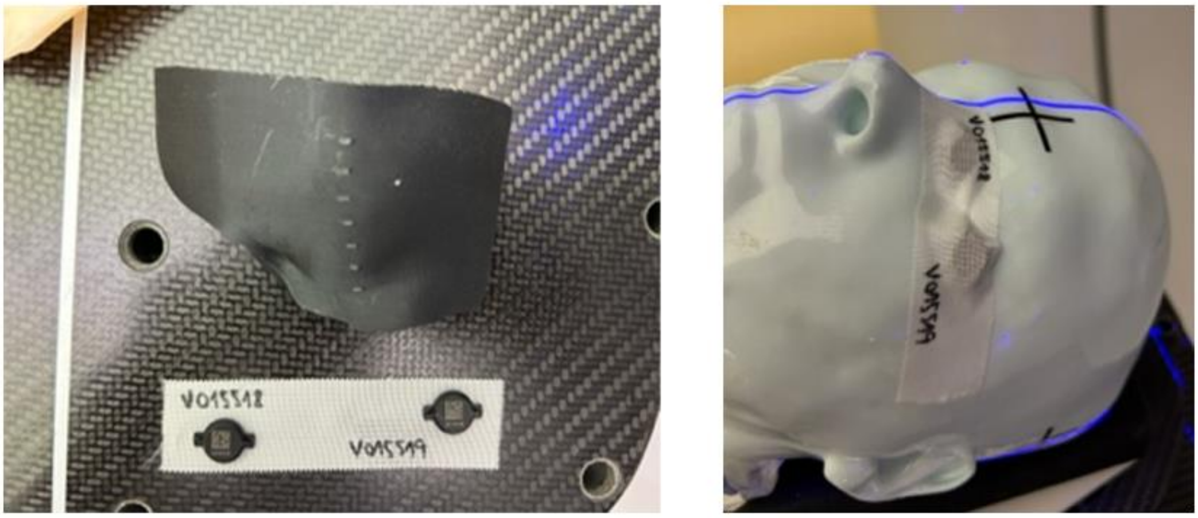

Figure 3.9 - a) 3D-printed bolus and BeOSL detectors; b) detectors positioning on phantom

The study found that the 3D-printed bolus effectively worked, with a 0.66% difference in dose between the TPS and OSL values, due to its lower air gap. The skin bolus had a larger dosage difference of 1.29%. However, the thermoplastic bolus was difficult to fit on the phantom, covering only part of the eye's surface. The irradiation dose was closely matched without the bolus exposure, suggesting the delivered dose may be incorrect.

Table 3.2 – Planning system vs detectors reported values

	3D-Printed Bolus		Skin Bolus		Thermoplastic Bolus	
mSv to cGy	Point 1	Point 2	Point 1	Point 2	Point 1	Point 2
TPS calculated dose	33.1	114.9	9.3	107.2	9.8	111.7
BeOSL measured dose	32.88	115.99	9.18	107.98	9.83	114.98
Difference (%)	0.66	0.94	1.29	0.72	0.30	2.89

The 3D-printed bolus was found to be accurate and met D50% limits within 2%. The skin bolus was better for filling the entire D50% area due to its flat outer area. The thermoplastic bolus had a high D50% dose variation due to its movement under the mask during setup. Accurate fitting and minimizing air gap are crucial for precise radiotherapy treatment. The bolus was also found to have optimal dose delivery for each form of bolus. To shape a thermoplastic bolus, it should be placed in a water bath at 65°C (149°F) to soften and then formed into the appropriate shape and thickness. Proper fitting and limiting air gap are essential for successful results in radiation applications. The 3D-printed bolus outperformed both commercial skin and thermoplastic boluses, highlighting the capability of 3D-printing technology to produce customized solutions for radiotherapy.

This part of the thesis was presented at several conferences, highlighting the research findings and their relevance to the field of radiation therapy. An oral presentation titled *"Assessing the Feasibility of 3D-Printed Bolus Materials for Clinical Radiation Therapy - Material Evaluation and Design Implementation on an Anthropomorphic Phantom"* was presented at the 9th National Congress of the Romanian Cancer Society's Federation, held in Cluj-Napoca from November 2-5, 2023, where it received the Best Physics Presentation Award. Accepted posters include *"Exploring the Impact of Filament Density on the Responsiveness of 3D-Printed Bolus Materials for High-Energy Photon Radiotherapy"*, presented at the ESTRO24 Congress in Glasgow, Scotland, from May 3-7, 2024 (published in Radiotherapy and Oncology, 194:S3258-S3261, DOI: 10.1016/S0167-8140(24)01774-2), and *"Dose Measurements and Design Implementation of 3D-Printed Bolus for Enhanced Radiotherapy Precision",* presented at ESTRO Meets Asia in Kuala Lumpur, Malaysia, from August 23-25, 2024 (published in Radiotherapy and Oncology, 197:S303-S304, DOI: 10.1016/S0167-8140(24)04066-0). Additionally, the findings were published in the paper titled "*Validation of a 3D Printed Bolus for Radiotherapy: A Proof-of-Concept Study",* available in Biomedical Physics & Engineering Express (Published February 12, 2025, A. C. Ciobanu et al., 2025, Biomed. Phys. Eng. Express 11 025033, DOI: 10.1088/2057-1976/adb15d, IF 1.3; AIS 0.279).

4. CHAPTER 4 - CLINICAL IMPLEMENTATION

4.1.Squamous cell carcinoma

Temporal bone carcinoma, which makes up 0.2% of head and neck cancers, is rare and often misdiagnosed due to common signs like ear pain and discharge. Late diagnosis of SCC worsens the prognosis, emphasizing the need for early identification. Squamous cell carcinoma in the middle ear is an unusual occurrence, as seen in a case of a 77-year-old male with blood-tinged otorrhea. The tumour was diagnosed as well-differentiated, and radical clearance after removal of the malleus and incus followed by radiotherapy ensured total remission. Early diagnosis and timely treatment are crucial for improved survival in cases of middle ear SCC.

4.1.1. Clinical case description

A 65-year-old female patient has been diagnosed with moderately differentiated squamous cell carcinoma of the right preauricular area, causing ulceration, bleeding, and invasion of the auricle and external auditory canal. The patient presents for radiation therapy and MRI imaging reveals a moderately infiltrative lesion in the external auditory canal and auricle, with right otomastoiditis and no lateral cervical adenopathy.

The patient has a moderately differentiated keratinized squamous cell carcinoma grade 2, with angioinvasion and undetermined neurotropism. Immunohistochemistry reveals HPV-associated cancer. The patient is advised to undergo conformal external beam radiation therapy, with a recommended dose of 50 Gy delivered in 25 sessions. A bolus is recommended for increasing the dose to the skin due to the superficial lesion.

4.1.2. Bolus design

A 3D-printed bolus was used to address intricate anatomical regions like the preauricular area and auditory canal. This method allows for customization to match patient anatomy contours, reducing air gaps and preserving thickness for efficient dose administration. The bolus required to extend into the auditory canal while covering the external ear highlighted the limitations of conventional methods. The scanning setup involved heating a 0.5 cm thermoplastic bolus, which was later modified to include the auditory canal. However, challenges included reducing the bolus's thickness to below 0.5 cm and causing air gaps, potentially compromising dose uniformity.

Thermoplastic bolus was tested for fit and functionality, but challenges such as thickness loss, air gaps, and repositioning made it difficult to reassemble the bolus. A 3D-printed bolus was chosen as a better alternative due to its ability to fit the ear and auditory canal easily, reducing the need for manual adjustments. This technique addresses issues of air gaps and thickness variations, providing a more consistent radiation therapy solution. The ear and auditory canal present unique challenges compared to other anatomical areas. The patient's DICOM files were acquired using a Siemens SOMATOM go.Top CT scanner, and a thermoplastic mask was used to immobilize the patient. The patient was positioned using a head and neck support system during the scan.

The process involved importing DICOM images and processing them using 3D Slicer. Segmentation was used to prevent model errors and maintain anatomical characteristics. Threshold segmentation values were used to avoid unnecessary scan areas. The topology of the model, consisting of triangles, quads, and N-gons, was smoothed to avoid surface imperfections and bumps while maintaining the ear and auditory canal anatomy.

A uniform thickness of 10 mm was applied to the bolus surface following the offset application. The design of the internal surfaces was especially focused on conformability to the ear and auditory canal without generating unequal layers or air gaps.

The solid STL model was used for 3D-printing of bolus designs due to their complexity. FDM printing was chosen over resin printing due to PLA's suitability, dimensional stability, and biocompatibility. PLA maintains its structural integrity throughout the printing process, unlike thermoplastic boluses that may lose thickness during hand shaping. This makes PLA a reliable choice for designing boluses in challenging anatomical areas.

The printed bolus underwent quality checks to ensure it matched the original design specifications. It was matched to the original CT scan data using 3D Slicer, and deviations were monitored to ensure the bolus accurately matched the anatomy. Approved by the multidisciplinary team, the bolus was ready for clinical use, providing a personalized, patient-specific solution for radiation therapy to the ear and auditory canal. This process illustrates how well we can produce highly accurate and repeatable bolus for difficult treatment locations with 3D-printing.

4.1.3. Treatment planning

The treatment for squamous cell carcinoma involved 50 Gy given in 25 fractions, following standard clinical guidelines. The dose constraints for organs at risk (OARs) were evaluated to ensure tolerance levels. The OARs were within the recommended tolerance levels, with the brain receiving a maximum dose of 45.5 Gy, the brainstem receiving a maximum dose of 12.5 Gy, and the optic chiasm receiving a maximum dose of 16.7 Gy. The treatment plan used Volumetric Modulated Arc Therapy (VMAT) to achieve the best dose distribution and coverage, resulting in 98.5% of the dose covering at least 95% of the target structure. The 3D mean dosage was 100.9%, and the maximum dose was 105.6%. The dose limits were successfully achieved for every critical structure, reducing the risk of radiation-induced side effects.

The PLA bolus ensured proper dose distribution by avoiding air gaps and providing consistent contact with the patient's anatomy. During CT simulation and treatment sessions, the patient was immobilized with a thermoplastic mask for stability, reducing movement and matching treatment sessions.

4.1.4. Results and follow-up

The patient demonstrated good tolerance to radiation treatment, with minimal side effects from 50 Gy delivered. 3D-printed PLA bolus improved tolerance by providing a customized experience with appropriate dose distribution and reducing exposure to adjacent organs. The radiation treatment plan prioritized the patient's quality of life during and after treatment.

A follow-up MRI scan confirmed a total response to radiation treatment for squamous cell carcinoma, indicating a significant shrinkage or no longer detectable tumour. This success highlights the need for customized treatment plans for complex cancer cases. The patient's tolerance and minimal side effects underscore the potency of radiation treatment and the importance of customized treatment in cancer therapy.

4.2. Total Scalp Irradiation (TSI)

4.2.1. Need of bolus for TSI

3D-printed bolus is a more efficient and accurate option for total scalp irradiation compared to thermoplastic or skin type bolus. Its high conformity and reproducibility ensure uniform dose distribution, minimizing the risk of underdosing or overdosing specific areas. 3D-printed bolus caps also provide better skin fit, resulting in more accurate dose delivery. Although it may require additional equipment and specialized expertise, advances in 3D-printing technology have reduced print times and improved workflow, making it a viable option for total scalp irradiation. The improved conformity, customization, reduced air gaps, dosimetric accuracy, and streamlined process make 3D-printed bolus a more favourable choice for optimizing treatment outcomes.

BASF Ultracur3D EL 4000 is a flexible, elastomeric resin developed by BASF Forward AM, a German manufacturer specializing in chemical products and 3D-printing materials. With a Shore hardness of 90 A, it offers superior strength, rebound, and tear resistance, making it suitable for various applications. Its excellent print quality and surface finish make it visually appealing. Available in transparent and black variants, it conforms well to complex shapes, making it suitable for close fit applications like cushioning pads. It can also be used to create patient-specific bolus caps for total scalp irradiation, ensuring a precise fit and optimal dose distribution.

It is important to note that the specific use of BASF Ultracur3D EL 4000 as a bolus for total scalp irradiation was subject to the clinical requirements and the preferences of the radiation therapy team.

4.2.2. Clinical case description

A 71-year-old woman with invasive lobular carcinoma underwent multiple mastectomy and lymphadenectomy. She was initially treated with adjuvant chemotherapy but refused radiotherapy. In January 2024, a right frontal metastasis was detected, leading to a gamma knife procedure and external beam radiotherapy. A palliative radiotherapy approach was proposed, involving total scalp irradiation from June 3 to June 20, 2024. The patient showed good tolerance to the treatment, but experienced hair loss and low-grade radiodermatitis. The case highlights the challenges of managing lobular carcinoma and the importance of personalized care and patient-centred treatment plans. The multidisciplinary approach required to address the disease's stages and metastases is highlighted.

4.2.3. Image processing and CT scanning setup

The workflow for DICOM and mesh handling involves determining the surface to be treated, such as a helmet-like printed part. The patient was scanned using Siemens SOMATOM go.Top CT, and machine tolerance and hair correction were necessary. Exporting the head to 3D STL format was insufficient, as it could create artifacts and generate inaccurate dimensions. The DICOM scan was imported into 3D Slicer, and threshold segmentation ranges were applied to find suitable values. The volume was rendered in 3D, and the model was exported to STL format.

The model was imported to Autodesk Fusion 360 after DICOM processing, but faced several faces and artifacts that couldn't be deleted in 3D Slicer. To prepare for surface modelling, a smoothing feature was applied to maintain mesh boundaries and patient head deviations. However, the model was not ready for printing due to surface imperfections or uneven thickness. A CAD approach was used to design the mesh, which was then processed and a quad topology applied to the body. A planar cut was made to maintain the physician's contoured shape, and an offset distance of 0.5 mm was applied to the surface.

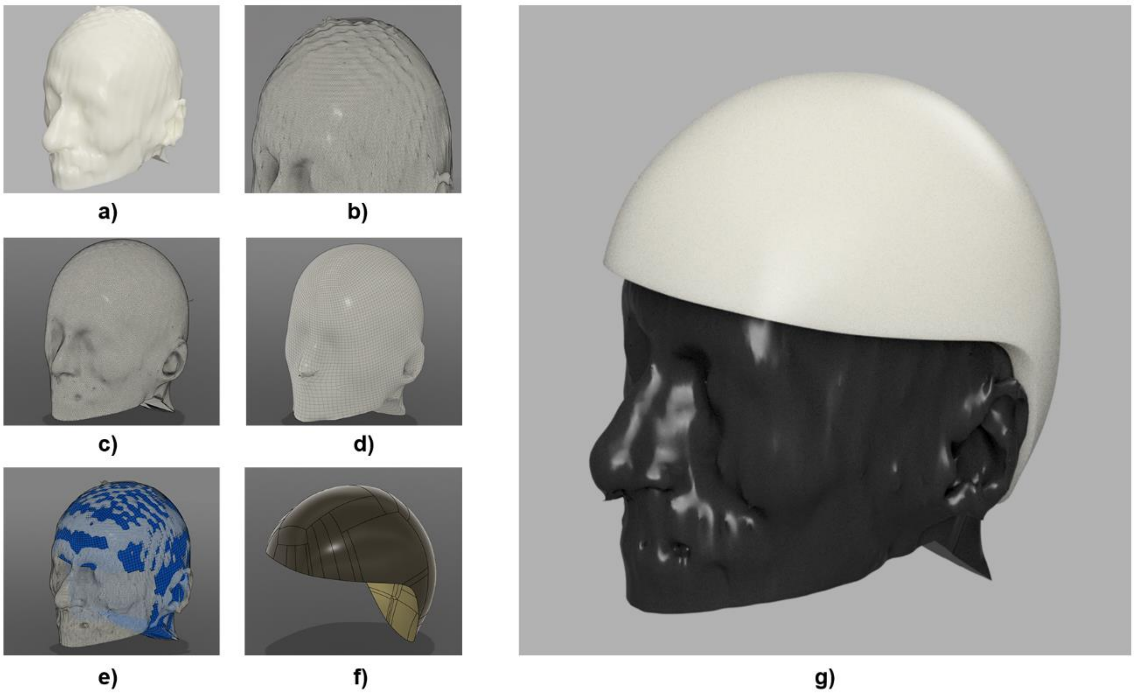

Figure 4.1 - a) Render version of the first phase of the model; b) Topology of the model (221 920 faces); c) Model after smoothing applied (102 640 faces); d) Quad topology (17 774 faces); e) Surface modelling (in blue – 6355 faces) comparted with the original mesh

The model was imported into 3D slicer for accuracy and multiple measurements techniques to identify errors. The solid model was exported into STL and processed using Lychee slicer software. A resin printing process was chosen over FDM printing due to good tolerances, curved surface support, flexile material, and uniform surface smoothing. The model was oriented with the exterior face to the build plate to avoid support interfaces with the patient head. CT simulation employed a 3mm head protocol and patient positioning for accurate imaging. A head and neck support system, headrest, and thermoplastic mask were used for stability and comfort. Arms were positioned near the body to minimize interference and maintain a consistent setup.

4.2.4. Treatment planning

The treatment planning for total scalp irradiation involved four coplanar full arcs to ensure optimal dose distribution coverage and preservation of organs-at-risk (OAR). The brain, eyes, and optic nerves were at risk due to potential complications such as cataracts and vision loss. The prescribed dose was initially 30 Gy in 10 fractions, but due to the patient's positive response, the total delivered dose was increased to 39 Gy in 13 fractions. The treatment plan resulted in a maximum dose of 107.1% of the prescribed total dose, which is considered acceptable according to the internal clinical protocol. The conformity index (CI) was calculated to be 0.95, assessing the degree to which the prescribed dose conforms to the target volume. The isodose level used to define the treated volume (TV) was the 98.85% isodose line, which aligns with the internal protocol's requirements for normalization ratio and maximum dose. The treated volume was approximately 299.7 cc, and the planning target volume (PTV) was 315.6 cc. The conformity index (CI) was calculated as the ratio of the treated volume to the PTV, resulting in a CI of 0.94986, within the acceptable range. The irradiation approach provided adequate dose coverage while minimizing exposure to surrounding healthy tissues.

Treatment planning aims to minimize radiation dose to healthy brain tissue while effectively treating the target area, minimizing long-term side effects and complications. Advanced techniques and technologies are used to deliver radiation precisely while sparing surrounding healthy tissues.

4.2.5. Results and follow-up

The treatment involved precise radiation delivery to targeted areas using a 3D-printed bolus cap and daily imaging, ensuring the plan was consistently aligned with the patient's specific needs.

The medical team optimized treatment outcomes by using a 3D-printed bolus cap for total scalp irradiation, ensuring precise and targeted radiation delivery. This approach, along with adherence to treatment guidelines and daily imaging, improved the patient's life expectancy and treatment precision. Despite expected side effects like hair loss and low-grade radiodermatitis, the overall benefits outweighed these temporary adverse reactions. This successful application of 3D-printed boluses in radiation therapy highlights their potential for enhancing treatment precision and patient outcomes.

This part of the thesis was presented at conferences, highlighting the clinical relevance and innovation of 3D-printed bolus applications in radiation therapy. An oral presentation titled "Total Scalp Irradiation with a 3D-Printed Bolus from Bench to Bedside" was presented at the 10th National Congress of the Romanian Cancer Society's Federation, held in Sinaia from October 24-27, 2024. A second presentation, "3D-Printed Bolus for Total Scalp Irradiation: A Case Study of a 71-Year-Old Woman with Metastatic Cancer", was presented at the Young Scientific Forum 2.0 in Poznan, Poland, on December 6, 2024.

The findings from this research are currently prepared for publication in the journal Technical Innovation and Patient Support in Radiation Oncology, under the title "Custom-Made, 3D-Printed Bolus Cap for a Case of Scalp Metastasis: A Single-Institution Study". This study highlights the feasibility of using patient-specific 3D-printed boluses for complex cases, demonstrating the transition of this innovative approach from experimental design to clinical application.

DISCUSSION

A study in Romania has demonstrated the superior adherence performance and patient-specific customization of 3D-printed boluses compared to traditional commercially available boluses. The results validate this hypothesis, demonstrating that 3D-printed boluses not only match depth dose distributions but also outperform them in reducing air gaps and ensuring uniform dose distribution, particularly over multiple treatment sessions. This research is the first clinical study on 3D-printed boluses in Romania, addressing a critical gap in the adoption of personalized radiation therapy in clinical practice. The study stands out by systematically evaluating various 3D-printed materials and providing a structured framework for material selection. The clinical cases investigated for total scalp irradiation and auricular carcinoma add new insights to the literature by tackling challenging treatment scenarios that have rarely been explored. The successful remission achieved in these cases underscores the potential of 3D-printed boluses to address complex clinical needs, bridging the gap between theoretical potential and practical application.

CONCLUSION

This PhD thesis explores the use of 3D-printed boluses in radiation therapy, focusing on material science, dosimetric validation, and clinical application. The research uses three core validation methods, each addressing critical aspects of bolus design, fabrication, and implementation. The results show that 3D-printed boluses offer a viable alternative to conventional materials, but challenges remain in standardization and clinical adoption. The first study evaluated the dosimetric properties of various 3D-printed materials, with polylactic acid (PLA) emerging as a leading candidate due to its favourable dose build-up and homogeneity. However, the study acknowledged the subjective nature of material selection and the need for expanded material ranges and printer-specific variables. The second validation method demonstrated superior anatomical conformity compared to thermoplastic and skin boluses, minimizing air gaps and improving dose distribution. The third method presented a novel 3D-printed PLA bolus for preauricular area and a 3D-printed bolus cap for total scalp irradiation, achieving complete remission in a patient with squamous cell carcinoma and multiple metastases. However, integrating 3D-printed boluses into routine practice requires addressing workflow bottlenecks, cost-effectiveness analyses, and solid quality control procedures.

LIST OF PUBLICATIONS

PUBLICATIONS ON THE TOPIC OF THE THESIS

1. Andreea-Cosmina Ciobanu, Lucian Cristian Petcu, Ferenc Járai-Szabó Szabo, Zoltán Balint. Exploring the impact of filament density on the responsiveness of 3D-Printed bolus materials for high-energy photon radiotherapy. European Journal of Medical Physics, November 1, 2024, doi: 10.1016/j.ejmp.2024.104849, Journal name European Journal of Medical Physics. AIS 0.677; IF 3.3, Q2
2. Andreea-Cosmina Ciobanu, Lucian Cristian Petcu, Ferenc Járai-Szabó Szabo, Zoltán Balint. Validation of a 3D printed bolus for radiotherapy: a proof-of-concept study. Biomedical Physics & Engineering Express, 11, February 12, 2025, doi: 10.1088/2057-1976/adb15d. Journal name: Biomedical Physics & Engineering Express. AIS 0.279; IF 1.3, Q3
3. Andreea-Cosmina Ciobanu, Virgil Sivoglo, Diana Maican, Ferenc Járai-Szabó Szabo, Zoltán Balint. Custom-made, 3D-printed bolus cap for a case of scalp metastasis: a single-institution study. Technical Innovations and Patient Support in Radiation Oncology. AIS 0.683; IF: 2.3 Q2

3 publications included in the thesis: total AIS = 1.639. 2 Q2; 1 Q3

OTHER PUBLICATIONS – CONFERENCE CONTRIBUTIONS

INTERNATIONAL CONFERENCES

1. Andreea-Cosmina Ciobanu, Mihaela Dumitru, Laura Rebegea, Ferenc Járai-Szabó Szabo, Zoltán Balint. Density on the Build-Up Region Responsiveness of 3D Printed Boluses in High-Energy Photon Radiotherapy, San Diego, California, October 1-4, 2023. Conference name: ASTRO Congress. Journal name: International Journal of Radiation Oncology, Biology, Physics, Volume 117, Issue 2, Supplement, Page e657 doi: 10.1016/j.ijrobp.2023.06.2089
2. Andreea-Cosmina Ciobanu, Lucian Cristian Petcu, Ferenc Járai-Szabó Szabo, Zoltán Balint. Exploring the impact of filament density on the responsiveness of 3D-Printed bolus materials for high-energy photon radiotherapy, Glasgow, Scotland, 3-7 May 2024. Conference name: ESTRO Congress. Journal name: Radiotherapy and Oncology, 194:S3258-S3261, doi: 10.1016/S0167-8140(24)01774-2

3. Andreea-Cosmina Ciobanu, Lucian Cristian Petcu, Adina Petcu, Florin Costache. Dose measurements and design implementation of 3D-Printed Bolus for enhanced radiotherapy precision, Kuala Lumpur, Malaysia, 23-25 August 2024. Conference name: ESTRO-meets-ASIA. Journal name: Radiotherapy and Oncology, 197:S303-S304, doi: 10.1016/S0167-8140(24)04066-0
4. Andreea-Cosmina Ciobanu, Ferenc Járai-Szabó Szabo, Zoltán Balint. A case study of a 71-year-old woman with metastatic cancer, Poznan, Poland, 6 December 2024, Conference name: Young Scientific Forum 2.0

NATIONAL CONFERENCES

1. Andreea-Cosmina Ciobanu, Mihaela Dumitru, Andreea Udrea, Madalina Eluta, Laura Rebegea. Dosimetric impact of bolus airgaps for clinical 6MV and 10MV photon beam, Sinaia, October 13-16, 2022. Conference name: Innovation and Multidisciplinarity in Cancer Treatment - Congress of the Romanian Radiotherapy Society
2. Andreea-Cosmina Ciobanu, Cristina Negoita, Mihaela Dumitru, Laura Rebegea. Bolus thickness influence in chest wall radiotherapy - Comparative study for no bolus, 0.5 cm bolus and 1 cm bolus, Bucharest, May 04-07, 2023. Conference name: Scientific Days of the Oncological Institute of Bucharest
3. Andreea-Cosmina Ciobanu, Florin Costache, Adina Petcu, Lucian Petcu. Assessing the Feasibility of 3D-printed Bolus Materials for Clinical Radiation Therapy - Material evaluation and design implementation on an anthropomorphic phantom, Cluj-Napoca, 2-5 November 2023. Conference name: From research to daily clinical practice sharing experience - The 9th National Congress of the Romanian Cancer Society's Federation
4. Andreea-Cosmina Ciobanu, Virgil Sivoglo, Zoltán Balint. Total Scalp Irradiation with a 3D-Printed bolus from bench to bedside, Sinaia, 24-27 October 2024. Conference name: The 10th National Congress of the Romanian Cancer Society's Federation